

1 **Application of far cortical locking technology in periprosthetic**
2 **femoral fracture fixation - a biomechanical study**

3
4 **Mehran Moazen, PhD¹**
5 **Andreas Leonidou, MSc²**
6 **Joseph Pagkalos, MSc²**
7 **Arsalan Marghoub, MSc¹**
8 **Michael J Fagan, PhD³**
9 **Eleftherios Tsiridis, MD, MSc, PhD, FRCS^{2,4,5}**

10
11
12
13
14 1. Department of Mechanical Engineering,
15 University College London,
16 Torrington Place, London WC1E 7JE, UK

17
18 2. Academic Orthopaedics and Trauma Unit,
19 Aristotle University Medical School,
20 University Campus 54 124, Thessaloniki, Greece

21
22 3. Medical and Biological Engineering,
23 School of Engineering,
24 University of Hull,
25 Hull, HU6 7RX, UK

26
27 4. Academic Department of Orthopaedic and Trauma,
28 University of Leeds,
29 Leeds, LS2 9JT, UK

30
31 5. Department of Surgery and Cancer, Division of Surgery,
32 Imperial College London,
33 London, W12 0HS, UK

34
35
36 **Corresponding author:**

37 Mehran Moazen, BSc, PhD, CEng, MIMechE, FHEA
38 Department of Mechanical Engineering,
39 University College London,
40 Torrington Place, London WC1E 7JE, UK
41 Tel: +44 (0) 208 954 0636
42 Fax: +44 (0) 208 954 6371
43 Email: Mehran_Moazen@yahoo.com; M.Moazen@ucl.ac.uk
44
45
46

Application of far cortical locking technology in periprosthetic femoral fracture fixation - a biomechanical study

Abstract

Background: Lack of fracture movement could be a potential cause of periprosthetic femoral fracture (PFF) fixation failures. This study aimed to test whether the use of distal far cortical locking screws reduce the overall stiffness of PFF fixations and allows an increase in fracture movement compared to standard locking screws while retaining the overall strength of the PFF fixations.

Methods: Twelve laboratory models of Vancouver type B1 PFFs were developed. In all specimens the proximal screw fixations were similar, while in six specimens distal locking screws were used, and in the other six specimens far cortical locking screws. The overall stiffness, fracture movement and pattern of strain distribution on the plate were measured in stable and unstable fractures under anatomical one-legged stance. Specimens with unstable fracture were loaded to failure.

Results: No statistical difference was found between the stiffness and fracture movement of the two groups in stable fractures. In the unstable fractures, the overall stiffness and fracture movement of the locking group was significantly higher and lower than the far cortical group, respectively. Maximum principal strain on the plate was consistently lower in the far cortical group and there was no significant difference between the failure loads of the two groups.

Conclusion: The results indicate that far cortical locking screws can reduce the overall effective stiffness of the locking plates and increase the fracture movement while maintaining the overall strength of the PFF fixation construct. However, in unstable fractures, alternative fixation methods e.g. long stem revision might be a better option.

73 **Keywords:** fracture stability, fracture movement, strain, stiffness, biomechanics,
74 Vancouver type B1, far cortical locking screw

75

76 **Running title:** Locking versus far cortical locking screw

77

78 **1. Introduction**

79 Periprosthetic femoral fractures (PFF) occur during or following total hip arthroplasty
80 (THA) [1-5]. It is likely that there will be an increase in the number of these fractures
81 as the number of THAs increases and the lifespan of patients increase [3].
82 Management of these fractures is challenging due to the presence of the underlying
83 prosthesis. With the introduction of locking plates and their advantage over
84 conventional non-locking plates, i.e. in preserving blood supply [6], their application in
85 the management of PFFs has increased [7, 8]. At the same time, there have been a
86 number of locking plate failures in PFF management [8-11]. Determining the reason
87 behind these failures is challenging. Three main factors are likely to be important: (1)
88 patient-specific factors such as fracture stability and bone quality [12,13]; (2) implant-
89 specific factors such as mechanical properties and design [14,15]; and (3) surgical
90 factors such as bridging length, method of application and fracture reduction [16,17].
91 Overall, it is widely accepted that both a lack or an excess of fracture movement,
92 dictated by the overall stiffness of the fracture fixation construct, will suppress callus
93 formation, and the fixation will ultimately fail due to high strain under cyclic loading
94 i.e. through mechanical fatigue [18,19].

95

96 It has been shown by several groups that locking plates can, depending on how they
97 have been applied, lead to overly rigid fixations that will suppress callus formation

98 [11,20]. Recently, Bottlang et al. [21] showed that far cortical locking screws, where
99 the screw locks into the plate and bypasses the near cortex, can reduce the effective
100 stiffness of locking plates compared to standard locking screws that are secured in
101 both near and far cortices. They demonstrated this in various laboratory models
102 replicating diaphyseal fracture fixation and in an animal model where distal and
103 proximal locking screws were compared versus far cortical locking screws [21-23].
104 Their results showed that far cortical locking screws: (1) reduce the overall stiffness
105 of the fracture fixation construct; (2) induce parallel fracture movement; (3) retain the
106 overall stiffness of the constructs; and (4) lead to a more uniform callus formation
107 than normal locking screws. Far cortical locking screws are now commercially
108 available and there is a growing body of literature on their applications [24, 25].

109

110 Considering the failure history of locking plates in PFF fixation and the introduction of
111 far cortical locking screws, this study was designed to test the application of the far
112 cortical locking screws in PFF fixations. The main aims of the study were to
113 understand to what extent distal far cortical locking screws: reduce the overall
114 stiffness; increase the fracture movement; alter the pattern of strain distribution on
115 the plate; and affect the overall strength of PFF fixations. Thus this study is
116 essentially asking the same questions as earlier studies that demonstrated the
117 innovation of far cortical locking screw in diaphyseal fracture fixation [21-23], but in
118 the context of PFF fixation. This is necessary because: (1) due to the presence of the
119 prosthesis, the load transfer path with PFF is different to that of an intact femur; (2) in
120 this study only distal far cortical screws are applied compared to proximal and distal
121 far cortical screws.

122

123 **2. Materials and methods**

124 **Specimens:** Twelve large, left, fourth-generation composite femurs (Sawbones
125 Worldwide, WA, USA) were used in this study with simulated Vancouver type B1
126 PFFs, i.e. with the fracture located around the stem with a stable implant and good
127 bone quality [1] fixation. The specimens were prepared by removing the femoral
128 condyles i.e. distal 60 mm of the femur. Then, total hip replacement was performed
129 using a Zimmer CPT femoral stem (Size 2) and Zimtron modular femoral head (28
130 mm diameter), both manufactured from stainless steel (Zimmer, IN, USA). The stem
131 was inserted into the femoral canal and cemented using Hi-Fatigue G Bone Cement
132 (Zimmer, Sulzer, Switzerland).

133

134 To minimize inter-specimen differences due to plate positioning and fracture
135 reduction, each specimen was plated first and then a simulated fracture was created
136 20 mm below the tip of stem using a band saw. A twelve hole titanium NCB
137 Periprosthetic Proximal Femur Plate (Zimmer, Warsaw, IN, USA) was used (length:
138 284 mm; thickness: 5 mm; width: 22 mm at the fracture site). The plate has a wide
139 section proximally and a narrow section distally. The wide section allows screw
140 insertion anterior and posterior to the underlying stem while the narrow section allows
141 single screw insertion (see Fig 1A). Six NCB (Non-Contact Bridging) screws were
142 used to fix the plate proximally (outer diameter: 4 mm; length: varying depending on
143 the location from 36-40 mm) while four screws were used distally (outer diameter: 5
144 mm; length: 40 mm). Three screw holes were left across the fracture gap equivalent
145 to a 100 mm bridging gap [17]. In all twelve specimens the proximal screw fixations
146 were similar, while in six specimens distal Locking screws (Zimmer, Warsaw, IN,
147 USA) were used, and in the other six specimens far cortical locking screws

148 (MotionLoc, Zimmer, Warsaw, IN, USA) were used (Fig 1B). All screws (proximal and
149 distal) were locked to the plate; the difference between the locking and far cortical
150 locking constructs was the bicortical fixation in the former, but only far cortical fixation
151 in the latter. During plating, spacers were used between the plate and bone to
152 provide a 1 mm plate-bone gap [26].

153

154 **Loading:** The distal 40 mm of the resected distal femur was fixed securely using
155 screws in a cylindrical housing and mounted on a material testing machine (Lloyd
156 Instruments, West Sussex, UK) at 10° adduction in the frontal plane and aligned
157 vertically in the sagittal plane [25,26]. This position simulates anatomical one-legged
158 stance [29]. Constructs were tested initially under axial loads of up to 700 N,
159 corresponding to recommended partial weight bearing i.e. toe touch weight bearing
160 [30]. Loading was applied to the femoral head stem via a hemispherical cup.

161

162 **Measurements:** The stiffness of the specimens was calculated from the slope of the
163 load-displacement data obtained from the material testing machine. Where there was
164 a bilinear stiffening effect, the initial, secondary and overall stiffness were reported.
165 The fracture movement was quantified using two micro-miniature differential variable
166 reluctance transducers (DVRT- LORD MicroStrain, VT, USA). The DVRTs were fixed
167 to the proximal and distal fragments of the fracture where the changes in the voltage
168 (due to displacement) were recorded in LabVIEW (National Instruments, TX, USA)
169 and converted to displacement based on separately calculated calibration data. The
170 accuracy of the DVRTs were 0.001 mm and were placed on the medial and lateral
171 sides of the femur across the fracture. The lateral DVRT was approximately 5 mm
172 from to the plate. The strain on the plate was recorded across the fracture site using

173 a Q100 Electronic Speckle Pattern Interferometry system (ESPI - Dantec Dynamics
174 GmbH, Ulm, Germany). The plate surface was first sprayed with a white spray to
175 create a non-reflective surface (DIFFU-THERM developer, Technische Chemie KG,
176 Herten, Germany). A three leg adaptor was fixed to the plate using X60 two
177 component adhesive (HBM Inc., Darmstadt, Germany) and was used to fix the Q100
178 sensor to the plate (Fig 1D). During the loading the speckle patterns were recorded
179 via the sensor and were used to calculate the displacement and strain at each
180 loading step using the Istra Q100 2.7 software (Dantec Dynamics GmbH, Ulm,
181 Germany). It must be noted that a preliminary test was conducted on an Aluminium
182 plate under tension where ESPI strain measurements across the plate were validated
183 against theoretical values. During the load-to-failure test, the first abrupt drop in the
184 load (obtained from the load-displacement data) was recorded as the initial crack
185 (typically seen to be a 17% drop in the load). Ultimate failure was recorded at the
186 point just before catastrophic failure of the construct, which coincided with complete
187 loss of loading (typically leading to a 50% drop in the load).

188

189 **Testing and analysis:** Specimens were first tested with a stable fracture where the
190 fracture gap produced by a band saw was filled with a similar sized slice of synthetic
191 bone. Overall stiffness and fracture movement were recorded for all specimens under
192 axial loading of 500 and 700 N. The lower value was selected to be consistent with
193 previous tests reported in the literature [28,31], however during preliminary tests it
194 was noted a change in slope of the load-deflection graph sometimes occurred at
195 typically 500 N therefore the test was extended to 700 N to capture that effect. The
196 sample with the closest stiffness to the average stiffness of all samples in each group
197 (i.e. locking and far cortical locking) was chosen for strain measurement on the plate

198 across the fracture site. Strain measurement was repeated five times and average of
199 the maximum (first) principal strain across the empty screw hole (averaged over the
200 whole surface as captured by the ESPI system in Fig 1D) was reported. Then, the
201 fracture gap in all samples was increased to 10 mm (i.e. unstable fracture - Fig 1C)
202 and same procedure was repeated. This enlarged gap was used to ensure that no
203 contact occurred at the fracture site under the initial loading up to 700 N, and was
204 similar to previous studies replicating commuted fractures [28, 31]. To ensure a like-
205 for-like comparison of the strain measurements, the same specimens used for the
206 strain measurement with stable fractures were re-used with unstable fracture (Fig
207 1D). Finally, all specimens with unstable fractures were loaded to failure. Two-tailed,
208 unpaired Student t-test at a level of significance of $p < 0.05$ was used to detect
209 significant differences in the stiffness, fracture movement and load-to-failure data. A
210 statistical analysis was not performed on the strain data since the strain
211 measurements were performed only on one specimen in each group.

212

213 **3. Results**

214 **Stiffness:** Under stable fracture conditions, the initial fracture gap (despite being
215 filled with a thin slice of synthetic bone) was seen to be fully closed at approximately
216 200 N in both the locking and far cortical locking groups (Fig 2A). As a result a
217 bilinear stiffness was observed for both locking (initial stiffness: 346 ± 149 N/mm;
218 secondary stiffness: 1194 ± 215 N/mm; overall stiffness of 660 ± 174 N/mm) and far
219 cortical locking group (initial stiffness: 314 ± 78 N/mm; secondary stiffness: 1273 ± 183
220 N/mm; overall stiffness: 640 ± 89 N/mm). No difference was detected between the two
221 groups in terms of any measures of fracture stiffness (Fig 3A).

222

223 Under unstable fractures (Fig 2B), a bilinear stiffness was again found in the locking
224 group at 200 N (initial stiffness: 345 ± 49 N/mm; secondary stiffness: 550 ± 48 N/mm;
225 overall stiffness: 443 ± 64 N/mm) and in the far cortical locking group at 500 N (initial
226 stiffness: 300 ± 38 N/mm; secondary stiffness: 458 ± 55 N/mm; overall stiffness: 331 ± 27
227 N/mm). The bi-linearity in the locking group appeared to occur as a result of plate-
228 bone contact at approximately 200 N, while in the far cortical locking group it was a
229 combined effect of far cortical locking screw bending and contacting the near cortex
230 and plate-bone contact. There were statistically significant differences between the
231 secondary ($p=0.011$) and overall ($p=0.003$) stiffnesses of the locking and far cortical
232 locking groups (Fig 3B).

233

234 **Fracture movement:** For the stable fracture condition, the lateral fracture movement
235 in both the locking and far cortical locking groups was less than 0.1 mm at 500 and
236 700 N. The medial fracture movement in the locking and far cortical locking groups
237 was 0.44 ± 0.2 mm and 0.63 ± 0.08 mm at 700 N, which were 23% and 11% higher
238 respectively than the 500 N values. There was no statistical difference between the
239 fracture movement between the two groups, however, the far cortical locking group
240 showed consistently higher fracture movement at both lateral and medial sides (Fig
241 4A).

242

243 In the unstable condition, the lateral fracture movement in both the locking and far
244 cortical locking groups ranged between 0.2-0.6 mm at 500 and 700 N. The medial
245 fracture movement in the locking and far cortical locking groups was 1.1 ± 0.2 mm and
246 1.6 ± 0.1 mm at 700N, 35% and 28% higher than 500 N values. There was a
247 statistically significant difference in fracture movement between the locking and far

248 cortical locking groups at both 500 N ($p=0.000$ at the lateral side; $p=0.003$ at the
249 medial side) and 700 N ($p=0.000$ at the lateral side; $p=0.001$ at the medial side),
250 where the far cortical locking group consistently showed higher fracture movement at
251 both lateral and medial sides (Fig 4B).

252

253 The ratio of lateral to medial fracture movement was calculated as an indicator of
254 parallel (i.e. axial) fracture movement across the fracture site. This ratio at 700 N for
255 the locking and far cortical locking group in the stable condition was 0.09 and 0.1
256 ($p=0.668$) while in the unstable condition was 0.24 and 0.37 ($p=0.005$) respectively
257 (based on Fig 4B).

258

259 **Strain:** In both the stable and unstable fractures, the overall pattern of maximum
260 principal strain on the plate across the empty screw hole was slightly lower in the far
261 cortical locking group compared to the locking group (Fig 5 and 6). A quantitative
262 analysis of the strain data showed that for a stable fracture, the maximum principal
263 strain in the locking group averaged over the surface that was captured by the ESPI
264 system (as shown in Fig 5 and 6) increased to 284 ± 27 μ S (microstrain) as the
265 loading increased to 700 N, while in the far cortical locking arrangement, the
266 maximum principal strain increased to 198 ± 41 μ S reaching a limit at 400 N (Fig 7A).
267 In the unstable fracture test, the maximum principal strain at 700 N was 809 ± 89 μ S
268 and 638 ± 40 μ S for the locking group and far cortical locking group respectively (Fig
269 7B).

270

271 **Failure:** During the failure tests, for all the locking screw specimens, crack initiation
272 and initial failure occurred at the closest screw to the fracture site on the proximal

273 femoral fragment (at 4656 ± 1067 N). The specimens eventually failed at the bone-
274 cement-stem interface at the proximal femur where the femoral stem dislocated (at
275 7217 ± 349 N - see Figs 8 and 9). Four of the far cortical locking specimens showed
276 initial cracks at an identical position to the locking specimens (at 6057 ± 923 N) and
277 eventually failed in a similar way to the locking specimens (at 7367 ± 1123 N - see Fig
278 9). One of the far cortical locking specimens failed at the base of the femur where the
279 construct was held in the cylindrical housing at 2778 N, and another far cortical
280 locking specimen failed at the most distal screw on the distal femoral fragment at
281 3630 N. Because they failed in a different way, these two samples were not included
282 in the data presented in Fig 9. No statistical difference was found in the failure results
283 between the locking and far cortical locking groups, regardless of whether the two
284 samples were included.

285

286 **4. Discussion**

287 Far cortical screws applied at both proximal and distal diaphyseal fragments have
288 been shown to increase fracture movement while retaining the overall strength of
289 fracture fixation constructs under pure axial, torsional and bending loads applied to
290 normal fracture specimens [21]. The current study tested whether the same was true
291 with periprosthetic femoral fractures where only distal far cortical locking screws were
292 applied, and the construct was loaded under an anatomically representative one-
293 legged stance. The results show similar findings to the previous study, i.e. distal far
294 cortical locking screws can reduce the overall stiffness of the locking construct and
295 increase the fracture movement while retaining the overall fixation construct strength.
296 However, the increase in the fracture movement and parallel fracture motion in the
297 far cortical locking group compared to the locking group recorded in this study was

298 not as high as that reported where both proximal and distal far cortical locking screws
299 were applied [21].

300

301 The far cortical locking screws only reduced the overall stiffness of fixation of the
302 unstable fractures. With a stable fracture, following the initial contact at the fracture
303 gap, no difference was observed between the far cortical locking and locking groups.
304 It is also noteworthy that the initial stiffness of the far cortical locking group was still
305 slightly lower than the locking group. However, in the unstable fracture, the far
306 cortical locking screws at the near cortex flexed elastically due to the enlarged gap,
307 delaying the plate-bone contact that occurred at the locking group at about 200 N,
308 and hence reduced the overall construct stiffness [see also 31]. Achieving a perfect
309 fracture reduction is clinically challenging and it is likely that in the majority of cases
310 there will be a small fracture gap remaining post-operatively. In these cases, the
311 constructs will behave in a more similar way to the unstable fracture group in this
312 study and, depending on the size of the gap, fracture stability will vary.

313

314 Medial fracture movement in the stable fracture group was in the range of ca. 0.2-0.6
315 mm while on the lateral side it was less than 0.1 mm. These movements are due to
316 inadequate fracture reduction, occurring here because of incomplete filling of the
317 initial fracture gap as described previously. The similarity between the initial stiffness
318 of the stable versus unstable fracture groups (for both the locking and far cortical
319 locking groups) confirms this. At the same time, while there was no statistical
320 significant difference between the fracture movement of the locking and far cortical
321 locking groups in the stable fractures, there was a significant difference between the
322 two groups in the unstable fractures. Considering the ratio of the lateral to medial

323 fracture movement as an indicator of parallel fracture movement, the far cortical
324 locking group showed higher parallel fracture movement i.e. 0.24 versus 0.37 at 700
325 N in the unstable fracture for locking and far cortical locking respectively (based on
326 Fig 4B). This was similar to the finding of Doornink et al. [23] who compared the far
327 cortical locking and locking screws in distal femoral fracture fixations. Their results
328 showed that at 800 N axial loading the lateral to medial fracture movement ratio was
329 0.53 and 0.90 for locking and far cortical locking respectively. The lower parallel
330 fracture movement in the far cortical locking group in this study compared to the
331 value reported by Doornink et al. [23] could be due to various differences between
332 the two studies. Nevertheless, higher parallel fracture movement in the far cortical
333 locking compare to locking screws has been shown to induce larger and more
334 uniform callus formation [22].

335

336 From a clinical point of view, considering that a titanium plate and screws were used
337 in this study and tested under post-operative load-bearing corresponding to toe touch
338 weight bearing, data obtained in this study suggests that: (1) with stable fractures,
339 application of far cortical locking screws can increase fracture movement; (2) with
340 unstable fractures or where large bridging lengths need to be considered, both
341 locking and far cortical locking screws can increase fracture movement beyond the
342 suggested threshold for healing i.e. 0.2-1 mm [18,19,32,33] and this effect could be
343 amplified at higher post-operative load bearings. Indeed, previous studies suggest
344 that in such cases, revision to a long stem or additional grafting might be a better
345 option [10, 34-36].

346

347 When the first principal strain on the plate across the empty screw holes are
348 considered, as expected, the strain in the stable fracture group was lower than the
349 unstable group. It was interesting that lower level of strain was recorded in the far
350 cortical locking group compare to the locking group (Fig 5 and 6). However, previous
351 finite element analysis studies [37,38] have shown that far cortical locking screws are
352 under higher strain compared to locking screws. Given the fracture movement data
353 obtained in this study and, in line with previous studies of Bottlang et al. [21, 22] for
354 stable fractures, it is possible that the fracture would heal before mechanical failure of
355 the screws. With the unstable fractures, the plate itself is under higher strain across
356 the empty screw holes. Nevertheless, the study of Bottlang et al. [25] did not show
357 either screw or plate failure in thirty-one distal fractures fixed with NCB Polyaxial
358 Locking Plate System and far cortical locking screws.

359

360 A consistent pattern of crack initiation at the closest screw to the fracture site on the
361 proximal femoral fragment was observed in the locking group and four of the far
362 cortical locking specimens. While previous finite element studies have shown high
363 stress concentration in this region on the bone, to the best of our knowledge most of
364 the clinical studies report failures of PFF fixations across the empty screw hole on the
365 plate [9-11]. This discrepancy is not unique to the present study, and is in fact
366 common between biomechanical studies [14,27].

367

368 There were several limitations in the present study that might have contributed to this
369 discrepancy. The properties of the composite femurs used in this study, could have
370 been higher than those observed clinically, especially in the case of osteoporotic
371 patients. Furthermore while the stiffness of these composite femurs may well be

372 optimised for general testing of implant performance, the many other characteristics
373 of bone, such as failure strength and screw pull-out strengths may not be. It is also
374 well established that *in vivo* bone responds to the mechanical strain, and such a
375 response together with the effect of muscle forces, knee joint movement and cyclic
376 loading that occurs *in vivo* were not included in this study. Acting in combination,
377 these factors could potentially lead to increased micromotion at the screw-bone
378 interface and higher implant strains *in vivo*, and care should therefore be taken in
379 their extrapolation to the clinical setting. However, the advantage of using these
380 composite femurs is that they are consistent with minimum variability between
381 individual bones, unlike natural femurs. Furthermore, any simplifications and
382 limitations in the study were the same for both the locking and far cortical locking
383 screws, therefore the relative comparisons made between the two screw designs in
384 the case of PFF fixations are likely to remain valid.

385

386 In conclusion, this study suggests that distal far cortical locking screws can reduce
387 the overall stiffness of the locking constructs in PPF fixation and increase the fracture
388 movement while retaining the overall construct strength. Further, it was found that in
389 unstable fractures, and where large bridging length are required, both locking and far
390 cortical locking screws applied with titanium plates might induce fracture movements
391 beyond the threshold required to promote callus formation, in which case long stem
392 revision might be a better option.

393

394

395 **References**

- 396 1. Duncan CP, Masri BA. Fractures of the femur after hip replacement. Instr Course
397 Lect 1995; 44:293-304.
- 398 2. Parvizi J, Rapuri VR, Purtill JJ, et al. Treatment protocol for proximal femoral
399 periprosthetic fractures. J Bone Joint Surg [Am] 2004;86:8-16.
- 400 3. Lindahl H, Malchau H, Oden A, et al. Risk factors for failure after treatment of a
401 periprosthetic fracture of the femur. J Bone Joint Surg [Br] 2006; 88:26-30.
- 402 4. Mont MA, Maar DC, Fractures of the ipsilateral femur after hip arthroplasty. A
403 statistical analysis of outcome based on 487 patients. J Arthroplasty 1994; 9:511-
404 9.
- 405 5. Inngul C, Enocson A, Postoperative periprosthetic fractures in patients with an
406 Exeter stem due to a femoral neck fracture: cumulative incidence and surgical
407 outcome. Int Orthop 2014; in press.
- 408 6. Perren SM. Evolution of the internal fixation of long bone fractures. The scientific
409 basis of biological internal fixation: choosing a new balance between stability and
410 biology. J Bone Joint Surg Br 2002;84:1093-110.
- 411 7. Niikura T, Sakurai A, Oe K, et al. Clinical and radiological results of locking plate
412 fixation for periprosthetic femoral fractures around hip arthroplasties: a
413 retrospective multi-center study. J Orth Sci 2014;19:984-90.
- 414 8. Graham SM, Moazen M, Leonidou A, et al. Locking plate fixation for Vancouver
415 B1 periprosthetic femoral fractures: A critical analysis of 135 cases. J Orth Sci
416 2013;18:426-36.
- 417 9. Buttaro MA, Farfalli G, Paredes Nunez M, et al. Locking compression plate
418 fixation of Vancouver type-B1 periprosthetic femoral fractures. J Bone Joint Surg
419 [Am] 2007; 89:1964-9.

- 420 10. Erhardt JB, Grob K, Roderer G, et al. Treatment of periprosthetic femur fractures
421 with the non-contact bridging plate: a new angular stable implant. Arch Orthop
422 Trauma Surg 2008;128:409-16.
- 423 11. Moazen M, Jones AC, Leonidou A, et al. Rigid versus flexible plate fixation for
424 periprosthetic femoral fracture - computer modelling of a clinical case. Med Eng
425 Phys 2012; 34:1041-8.
- 426 12. Claes L, Eckert-Hubner K, Augat P. The fracture gap size influences the local
427 vascularization and tissue differentiation in callus healing. Langenbecks Arch
428 Surg 2003; 388:316-22.
- 429 13. Leonidou A, Moazen M, Lepetsos P, et al. The biomechanical effect of bone
430 quality and fracture topography on locking plate fixation in periprosthetic femoral
431 fractures. Injury 2015; 46:213-17.
- 432 14. Lenz M, Gueorguiev B, Joseph S, et al. Angulated locking plate in periprosthetic
433 proximal femur fractures: biomechanical testing of a new prototype plate. Arch
434 Orthop Trauma Surg 2012;132:1437-44
- 435 15. Wahnert D, Schroder R, Schulze M, et al. Biomechanical comparison of two
436 angular stable plate constructions for periprosthetic femur fracture fixation. Int
437 Orthop 2014;38:47-53.
- 438 16. Dennis MG, Simon JA, Kummer FJ, et al. Fixation of periprosthetic femoral shaft
439 fractures occurring at the tip of the stem: a biomechanical study of 5 techniques. J
440 Arthroplasty 2000;15:523-8.
- 441 17. Stoffel K, Dieter U, Stachowiak G, et al. 2003. Biomechanical testing of the LCP--
442 how can stability in locked internal fixators be controlled? Injury 2003;34 Suppl
443 2:B11-9.

- 444 18. Goodship AE, Kenwright J. The influence of induced micromovement upon the
445 healing of experimental tibial fractures. *J Bone Joint Surg [Br]* 1985; 67:250-5.
- 446 19. Augat P, Merk J, Ignatius A, et al. Early, full weight bearing with flexible fixation
447 delays fracture healing. *Clin Orthop Relat Res* 1996; 328:194-202.
- 448 20. Lujan TL, Henderson CE, Madey SM, et al. Locked plating of distal femur fracture
449 leads to inconsistent and asymmetric callus formation. *J Orthop Trauma* 2010;
450 24:156-62.
- 451 21. Bottlang M, Doornink J, Fitzpatrick DC, et al. Far cortical locking can reduce
452 stiffness of locked plating constructs while retaining construct strength. *J Bone*
453 *Joint Surg Am* 2009;91:1985-94.
- 454 22. Bottlang M, Doornink J, Lujan TJ, et al. Effects of construct stiffness on healing of
455 fractures stabilized with locking plates. *J Bone Joint Surg [Am]*. 2010;92:12-22.
- 456 23. Doornink J, Fitzpatrick DC, Madey SM, et al. Far cortical locking enables flexible
457 fixation with periarticular locking plates. *J Orthop Trauma* 2011; 25:S29-S34.
- 458 24. Ries Z, Hansen K, Bottlang M, et al. Healing results of periprosthetic distal femur
459 fractures treated with far cortical locking technology: a preliminary retrospective
460 study. *Iowa Orthop J* 2013;33:7-11.
- 461 25. Bottlang M, Fitzpatrick DC, Sheerin D, et al. Dynamic fixation of distal femur
462 fractures using far cortical locking screws: a prospective observational study. *J*
463 *Orthop Trauma* 2014;28:181-8.
- 464 26. Ahmad M, Nanda R, Bajwa AS, et al. Biomechanical testing of the locking
465 compression plate: When does the distance between bone and implant
466 significantly reduce construct stability? *Injury* 2007; 38:358-64.
- 467 27. Zdero R, Walker R, Waddell JP, et al. Biomechanical evaluation of periprosthetic
468 femoral fracture fixation. *J Bone Joint Surg [Am]* 2008; 90:1068-77.

- 469 28. Moazen M, Jones AC, Jin Z, et al. Periprosthetic fracture fixation of the femur
470 following total hip arthroplasty: a review of biomechanical testing. Clin Biomech
471 2011; 26:13-22.
- 472 29. Bergmann G, Deuretzbacher G, Heller M, et al. Hip contact forces and gait
473 patterns from routine activities. J Biomech 2001; 34:859-71.
- 474 30. Ryf CR, Arraf J: Postoperative fracture treatment: general considerations. p. 447.
475 In Ruedi TP, Buckley RE, Moran CG, eds. AO principles of fracture management,
476 2ed. Davos: AO Publishing; 2007.
- 477 31. Moazen M, Mak JH, Etchells LW, et al. The effect of fracture stability on the
478 performance of locking plate fixation in periprosthetic femoral fractures. J
479 Arthroplasty 2013;28:1589-95.
- 480 32. Egol KA, Kubiak EN, Fulkerson E, et al. Biomechanics of locked plates and
481 screws. J Orthop Trauma 2004; 18:488-93.
- 482 33. Claes L, Wilke H-J, Augat P, et al. Effect of dynamization of gap healing of
483 diaphyseal fractures under external fixation. Clin Biomech 1995; 8:227-34.
- 484 34. Haddad FS, Duncan CP, Berry DJ, et al. Periprosthetic femoral fractures around
485 well-fixed implants: use of cortical onlay allografts with or without a plate. J Bone
486 Joint Surg [Am] 2002; 84:945-50.
- 487 35. Moazen M, Mak JH, Etchells LW, et al. Periprosthetic femoral fracture - a
488 biomechanical comparison between Vancouver type B1 and B2 fixation methods.
489 J Arthroplasty 2014;29(3):495-500.
- 490 36. Sariyilmaz K, Dikici F, Dikmen G, et al. The Effect of Strut Allograft and Its
491 Position on Vancouver Type B1 Periprosthetic Femoral Fractures: A
492 Biomechanical Study. J. Arthroplasty 2014;29:1485-90.

493 37. Bottlang M, Feist F. Biomechanics of far cortical locking. J Orthop Trauma
494 2011;25 Suppl 1:S21-8.

495 38. Moazen M, Mak JH, Jones AC, et al. Evaluation of a new approach for modelling
496 the screw–bone interface in a locking plate fixation - a corroboration study. Proc
497 Inst Mech Eng H 2013;227:746-56.

498

499

500

501

502

503

504

505

506

507

508

509

510

511

512

513

514

515

516

517

518 **Figure legends**

519 **Fig. 1** An overview of the study: (A) lateral view of the plate and anterior-posterior
520 radiograph of a locking periprosthetic femoral fracture fixation construct; (B)
521 comparing distal Locking versus Far cortical locking screws; (C) comparing stable
522 versus unstable fractures; (D) a summary of the parameters recorded in this study,
523 also highlighting the electronic speckle pattern interferometry sensor (attached to the
524 plate) and micro-miniature differential variable reluctance transducers (attached to
525 the bone).

526

527 **Fig. 2** Graph of the load-displacement data recorded under stable (A) and unstable
528 (B) fractures for the locking and far cortical locking group.

529

530 **Fig. 3** Summary of the initial, secondary and overall stiffness values calculated under
531 stable (A) and unstable (B) fractures for the locking and far cortical locking groups. *
532 highlight statistical significance between the corresponding groups ($p < 0.05$).

533

534 **Fig. 4** Summary of the fracture movement data under stable (A) and unstable (B)
535 fractures for the locking and far cortical locking groups at the lateral (lat) and medial
536 (med) side at 500 and 700 N. * highlight statistical significance between the
537 corresponding groups ($p < 0.05$).

538

539 **Fig. 5** Comparison between the pattern of maximum principal strain across the empty
540 screw hole on the fracture plate, between the locking and far cortical locking group
541 for stable fractures at 500 and 700 N.

542

543 **Fig. 6** Comparison between the pattern of maximum principal strain across the empty
544 screw hole on the fracture plate, between the locking and far cortical locking group
545 for unstable fractures at 500 and 700 N.

546

547 **Fig. 7** Summary of the average maximum principal strain across the empty screw
548 hole on the fracture plate for the locking and far cortical locking group under stable
549 (A) and unstable (B) fracture conditions during loading up to 700 N.

550

551 **Fig. 8** An example of a locking sample load to failure test, highlighting the crack
552 initiation at about 4000 N and ultimate failure at about 6900 N.

553

554 **Fig. 9** Summary of the load to failure data, highlighting the crack initiation and
555 ultimate failure loads of the unstable fractures for the locking and far cortical locking
556 groups. No statistical difference was observed between the aforementioned groups.

557

558

559

560

561

562

563

564

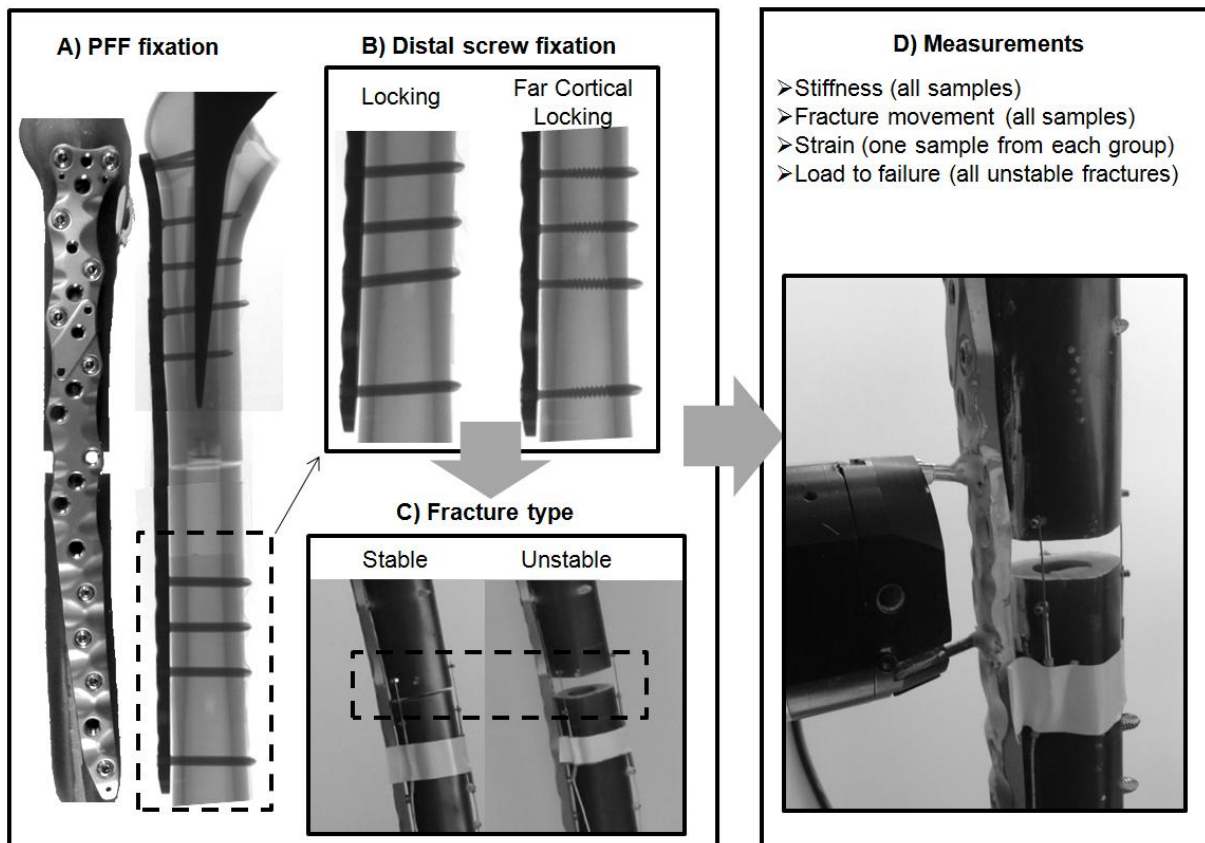
565

566

567

568

Fig 1



570

571

572

573

574

575

576

577

578

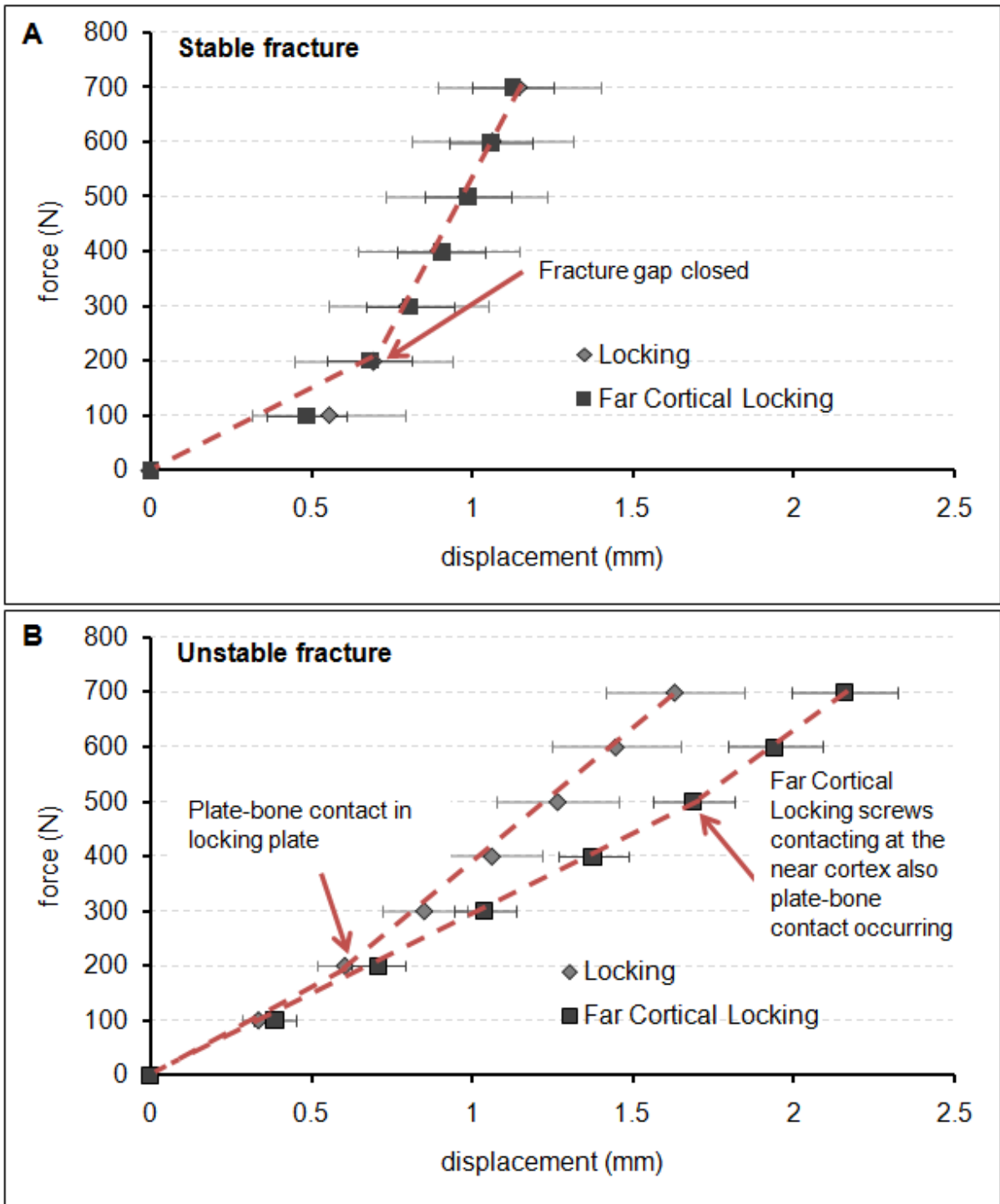
579

580

581

582

583 **Fig 2**



584

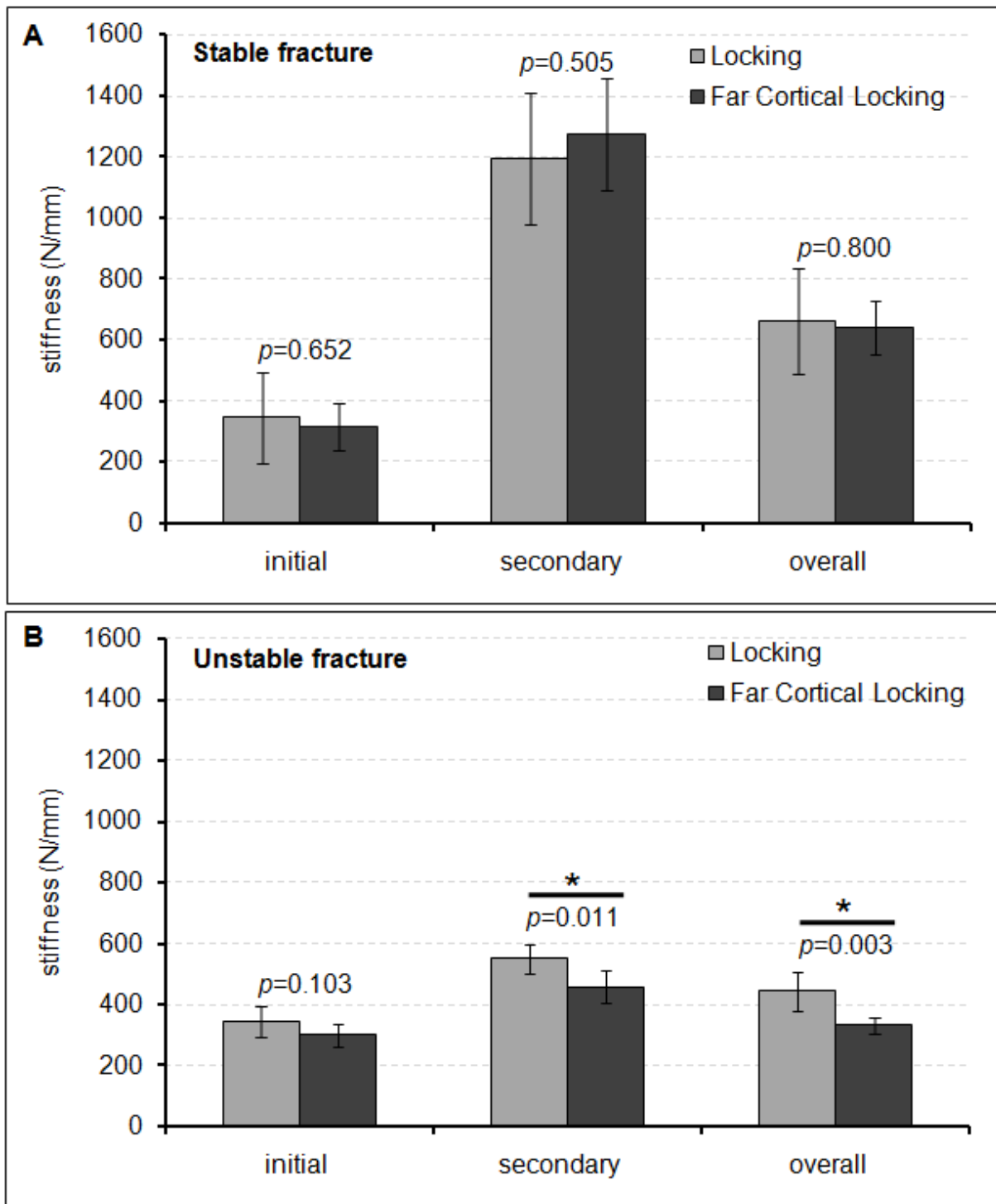
585

586

587

588

589 **Fig 3**



590

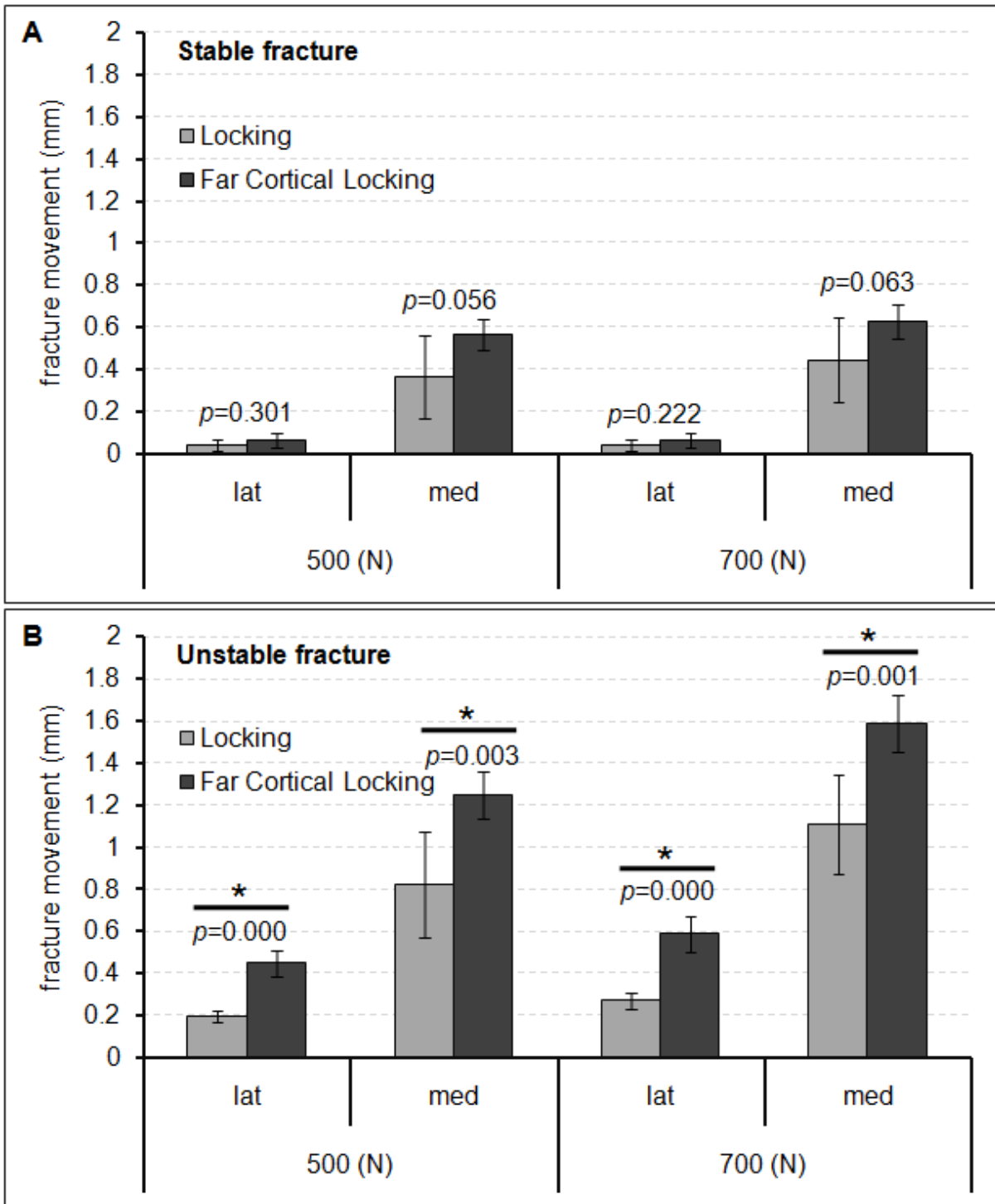
591

592

593

594

595 **Fig 4**



596

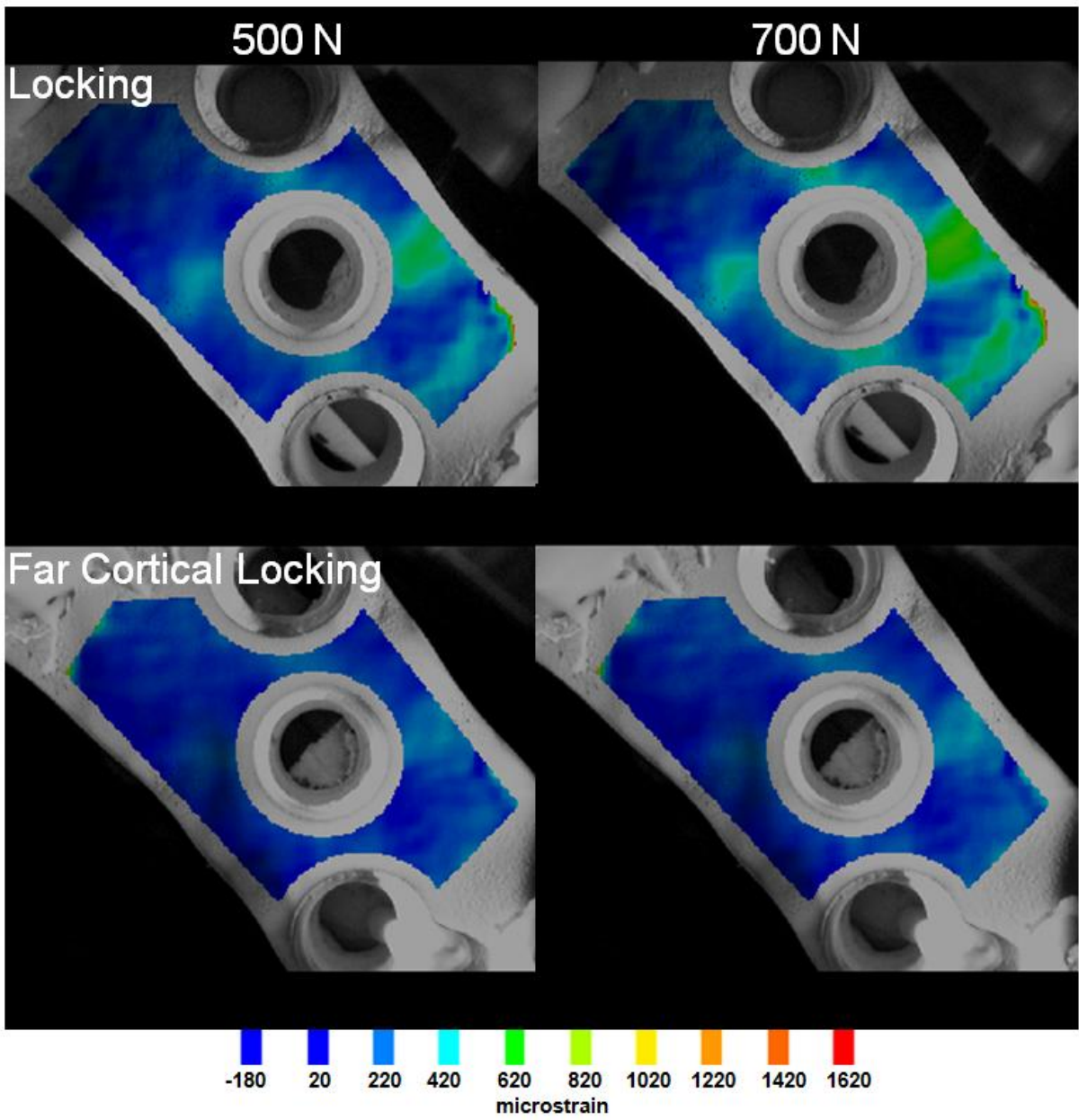
597

598

599

600

601 **Fig 5**



602

603

604

605

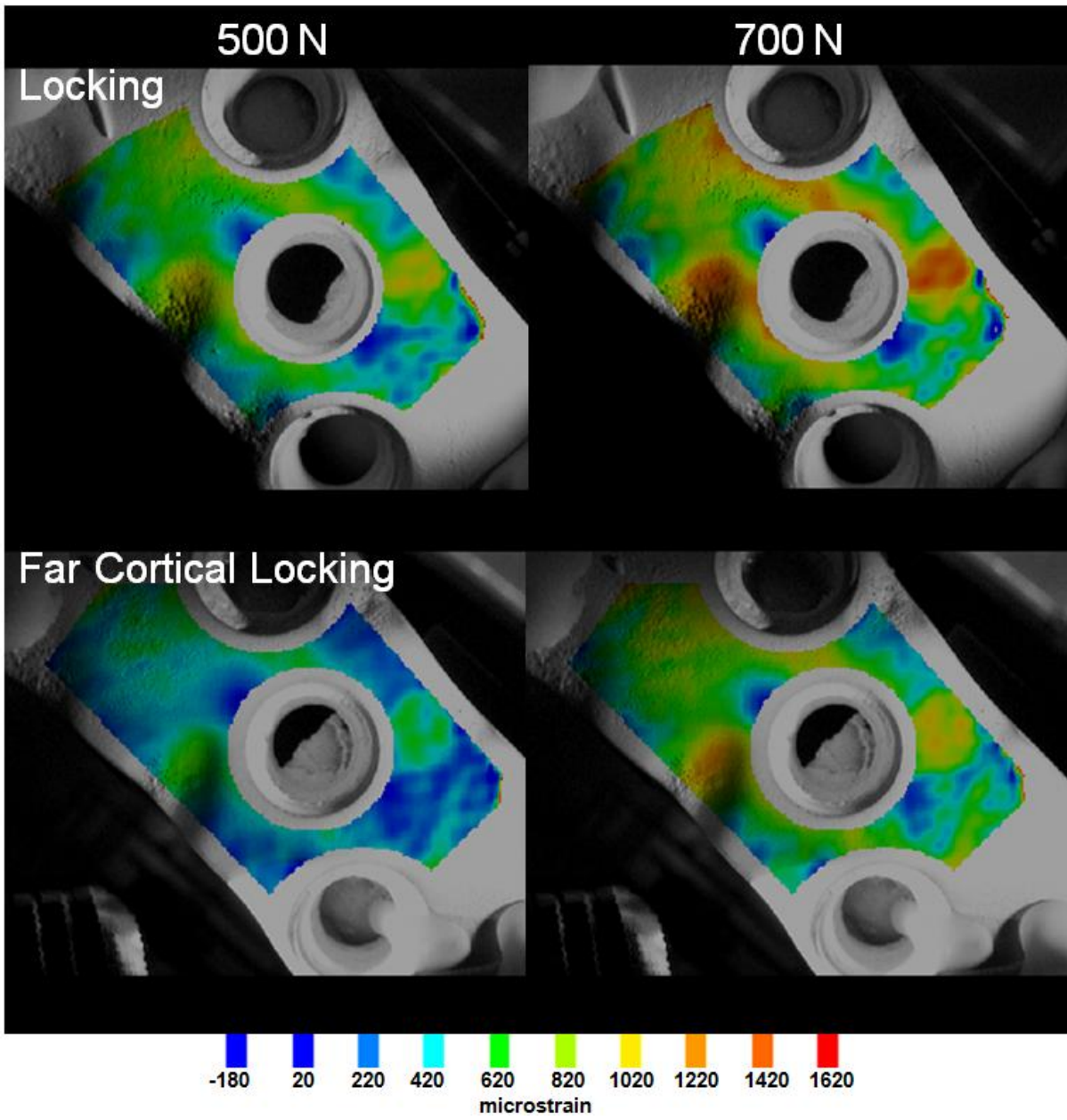
606

607

608

609

610 **Fig 6**



611

612

613

614

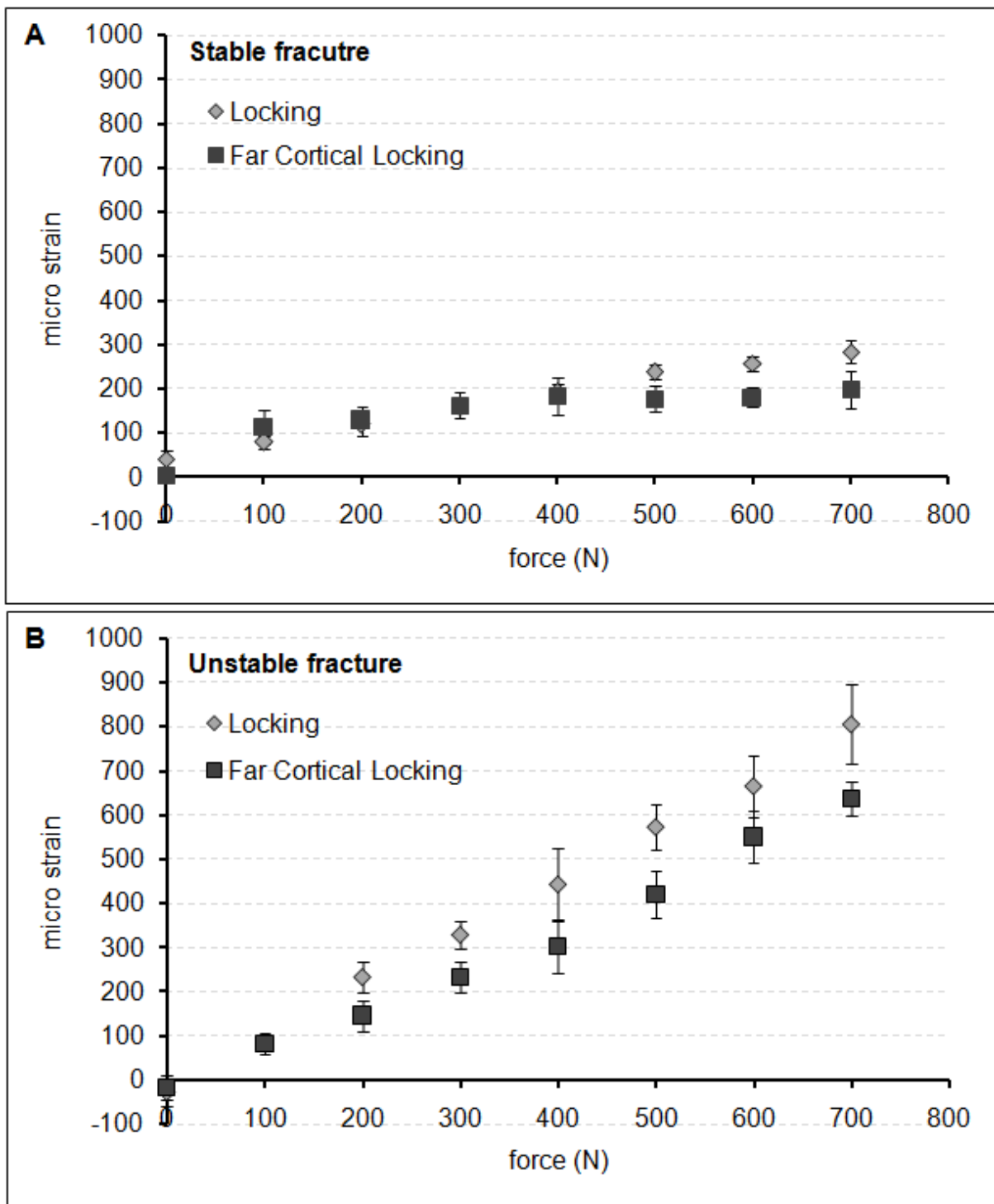
615

616

617

618

619 **Fig 7**



620

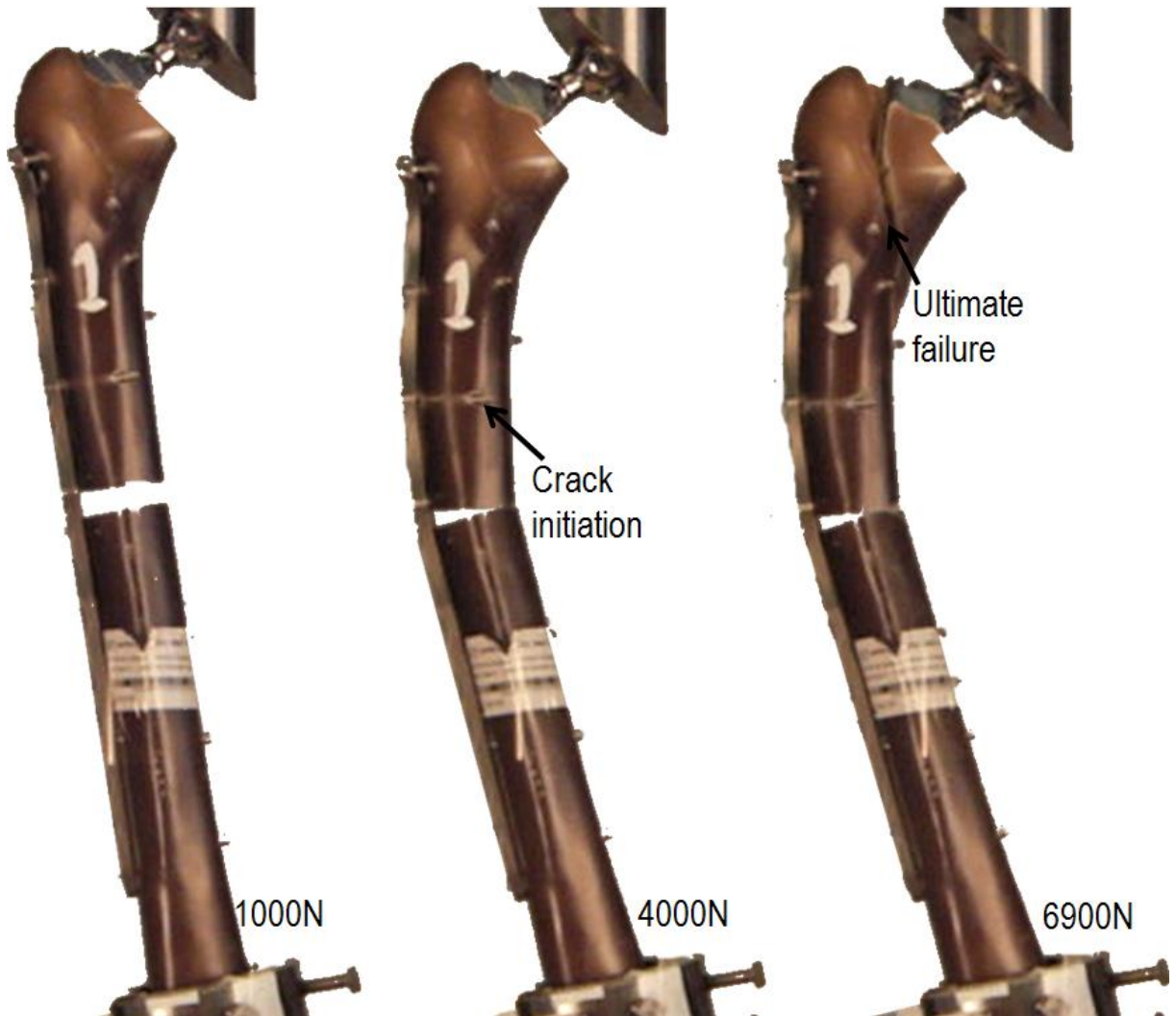
621

622

623

624

625 **Fig 8**



626

627

628

629

630

631

632

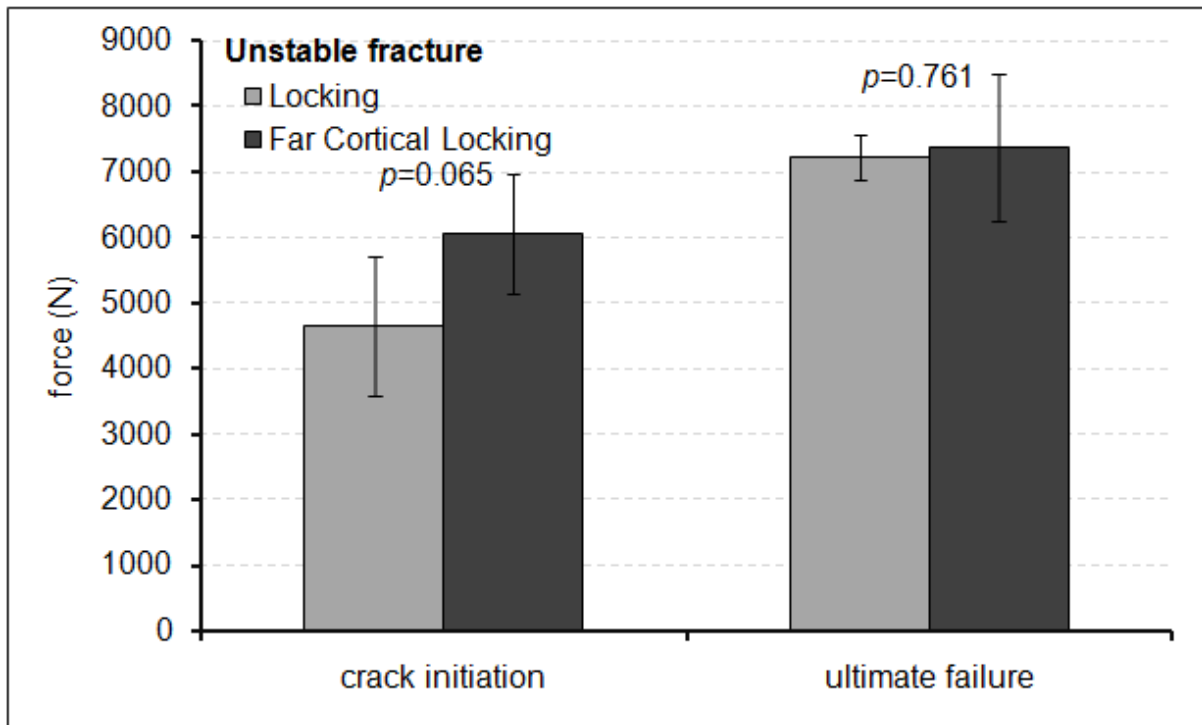
633

634

635

636

637 **Fig 9**



638